frontiers | Frontiers in Earth Science

TYPE Policy and Practice Reviews
PUBLISHED 09 January 2023
DOI 10.3389/feart.2022.1042371

OPEN ACCESS

EDITED BY
Shaohong Xia,
South China Sea Institute of Oceanology (CAS), China

REVIEWED BY
Xiaoxiao Yu,
Guangzhou Institute of Geochemistry (CAS), China
Luigi Jovane,
University of São Paulo, Brazil

*CORRESPONDENCE
S. Wu,
swu@idsse.ac.cn

SPECIALTY SECTION
This article was submitted to Marine Geoscience, a section of the journal Frontiers in Earth Science

RECEIVED 12 September 2022
ACCEPTED 17 November 2022
PUBLISHED 09 January 2023

CITATION
Liu Y, Wu S, Li X, Chen W, Han X, Yang C, Qin Y, Huang X, Yang Z, Sun J and Zhu L (2023), Seismic stratigraphy and development of a modern isolated carbonate platform (Xuande Atoll) in the South China Sea.
Front. Earth Sci. 10:1042371.
doi: 10.3389/feart.2022.1042371

Seismic stratigraphy and development of a modern isolated carbonate platform (Xuande Atoll) in the South China Sea

Y. Liu[1,2], S. Wu[1,2,3]*, X. Li[1,4], W. Chen[1,2], X. Han[5], C. Yang[5], Y. Qin[1], X. Huang[1,6], Z. Yang[7], J. Sun[1] and L. Zhu[1]

[1]Laboratory of Marine Geophysics and Georesources of Hainan Province, Institute of Deep-Sea Science and Engineering (CAS), Sanya, China, [2]School of Earth Sciences, University of Chinese Academy of Sciences, Beijing, China, [3]Laboratory for Marine Geology, Qingdao National Laboratory for Marine Science and Technology, Qingdao, China, [4]Sanya Institute of South China Sea Geology, Guangzhou Marine Geological Survey, Sanya, China, [5]Marine Geological Survey Institute of Hainan Province, Haikou, China, [6]Institute of Earth and Environmental Science, University of Potsdam, Potsdam, Germany, [7]Institute of Georesource, Guangzhou Marine Geology Survey, Guangzhou, China

Xuande Atoll is an isolated carbonate platform that has developed since the early Miocene. This study conducted high-resolution seismic surveys and shallow drilling to understand its internal structure and development. Five seismic sequences were observed (from bottom to top): SQ1 (early Miocene), SQ2 (middle Miocene), SQ3 (late Miocene), SQ4 (Pliocene), and SQ5 (Quaternary). The seismic data indicated that the platform formation started in the early Miocene and flourished during the early and middle Miocene. The platform shrank before the isolated platform formed in the middle Miocene. The final shrinking stage occurred in the southern and western parts of the platform at the end of the Miocene, which may reflect rapid tectonic subsidence and increased terrigenous sediment inputs owing to the formation of the semi-marginal sea. The peri-platform contains a falling sea-level sequence that was dominated by mass wasting deposits.

KEYWORDS

carbonate platform, tectonic control, monsoon, coral atoll, Xisha

Introduction

Siliciclastic sequence stratigraphy on continental margins has constrained the lateral contrasts from shelf to deep-water basin facies, which usually comprise lowstand, transgressive, and highstand sequences controlled by changes in sea level (Mitchum Jr et al., 1977; Vail et al., 1977; Van Wagoner et al., 1987; Jervey, 1988; Posamentier and Vail, 1988; Sarg, 1988; Jovane et al., 2016). However, the sequence stratigraphy of carbonate margins is not entirely understood, particularly on modern isolated platforms. The sequence and structure of the isolated carbonate platform are controlled by various factors, including tectonics, sea levels, carbonate productivity, terrigenous sediment

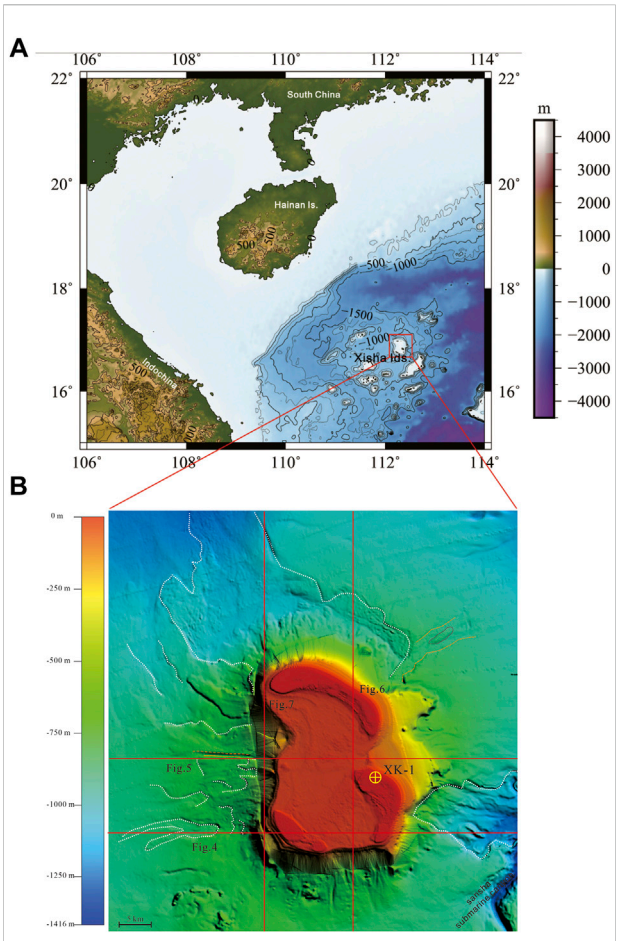

FIGURE 1
Geomorphology and seismic line location. **(A)** Bathymetric map of the northern South China Sea. **(B)** Bathymetric map of Xuande Atoll. Water depths in the reef flat were measured using a single-beam system, while the deepwater data were obtained using a multi-beam system. Red lines: multi-channel seismic (MCS) survey lines; circles: drilled holes.

inputs, and marine palaeoceanography (Eberli and Ginsburg, 1987; Wilson, 2002; Wilson, 2008; Betzler et al., 2009; Schlager and Warrlich, 2010). The structure of tropical carbonate sequences depends not only on relative decreases in sea level but also on the reef production rate, erosion rate, and accommodation space. Generally, no apparent lateral variations are observed in the reef flat but can be observed in falling sea level tracts (FSTs) on the reef slope, including strong gravity flow and bottom current deposits. Sea level, coral reef growth, and palaeoceanography also affect the structure of tropical carbonate platforms. A carbonate platform can produce debris that is then transported to the deepwater slope by gravity flow (Wilson, 2002; Fournier et al., 2004; Wilson, 2008; Schlager and Warrlich, 2010).

Although seismic imaging of drowned or buried isolated carbonate platforms has been conducted in the Gulf of Papua New Guinea, Northeast Australia, Great Bahama Bank, and Southeast Asia (Ludmann et al., 2005; Tcherepanov et al., 2008; Wu et al., 2014), only a few high-resolution seismic surveys of the shallow lagoon and reef flat have been performed. In particular, few multi-channel seismic (MCS) surveys have been performed on most modern carbonate platforms, which are common in the Xisha archipelago in the South China Sea (SCS) (Wu et al., 2014; Shao et al., 2017).

Xuande atoll is located in the east of the Xisha archipelago. Previous studies have described the development of Xuande Atoll based on lithological observations, sedimentary facies analysis, thin section identifications, and geochemical analyses of samples from drilled wells (Shao et al., 2017). However, as all these wells were drilled on the Yongxing Island of Xuande Atoll, the results only reflect vertical facies variations; thus, the three-dimensional structure of the platform remains unclear. We conducted four seismic survey lines across Xuande Atoll in the Xisha archipelago in 2017 (Figure 1). In this study, we report on newly collected data from seismic surveys and holes drilled across Xuande Atoll. We investigated the three-dimensional growth of the platform using seismic and well data to determine the development of this modern isolated carbonate platform to improve our current understanding of modern carbonate platform development and determine the sequence stratigraphy and evolution of Cenozoic platforms (Figure 1).

Geologic setting

The Xisha archipelago is located on the continental slope of the SCS margin, which has been undergoing continental rifting, subsequent extension, and post-extensional drift since the late Cretaceous (Figure 1). The timing of the seafloor spread has recently been revised from 33 to 23.6 Ma in the northwest sub-basin and from 23.6 to 15 Ma in the east sub-basin, using data from the International Ocean Discovery Project (IODP) Site U1435 (Taylor and Hayes, 1980; Briais et al., 1993a; Cullen, 2010; Li et al., 2015). Tectonically, the Xisha archipelago is part of the Xisha uplift, which was formed by Palaeocene hyper-extended rifting bounded by high-angle faults (Tapponnier et al., 1982a; Qiu et al., 2001; Hall, 2002; Li et al., 2015). Since the late early Miocene, the regional tectonics have comprised a post-rifting setting characterised by thermal subsidence (Wu et al., 2009). In addition, the acoustic basement of the uplift is Precambrian grey granite gneiss and Mesozoic volcanic rocks, as determined from data from well XY-1 (Wang et al., 1979; Qiu et al., 2006). Recently, well XK-1 encountered metamorphic rocks and granite basement at depths of 1257.52–1268.02 m, comprising late Jurassic adamellites (152 ± 1.7 Ma) and Cretaceous granites (107.8 ± 3.6 Ma) (Zhu et al., 2017). The basement observed in well XK-1 could be volcaniclastic rocks (36.01 ± 0.59–37.68 ± 1.37 Ma) and Yanshanian granitic rocks (105.73 ± 1.39–146.10 ± 1.73 Ma), as well as scattered Precambrian crystalline basement

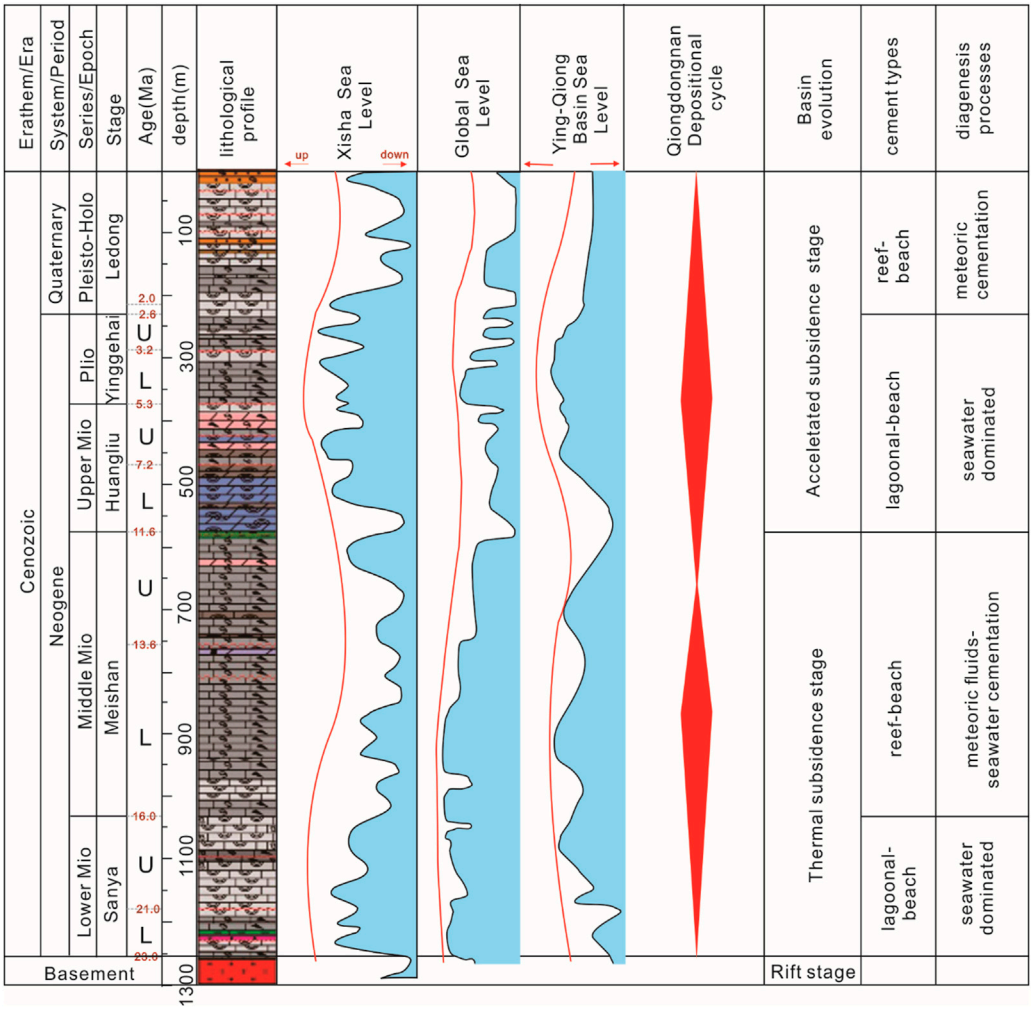

FIGURE 2
Stratigraphic contrasts in well XK-1 on Yongxing Island at Xuande Atoll (Shao et al., 2017). The drilling site is shown in Figure 1.

(623.40 ± 6.67–884.1 ± 7.70 Ma). Owing to the stable tectonic setting associated with the steep incline generated in the Palaeocene, the Xisha platform initiated in the early Miocene and has remained active to the present (Ma et al., 2011; Wu et al., 2014; Shao et al., 2017).

The geomorphology of Xuande Atoll has recently been investigated using dense single-beam bathymetric measurements of the reef flat and multi-beam bathymetry of the lower slope (Figure 2). Three coral reef flats are present on the huge reef platform, including Qilianyu shoal, Yongxing Island, and Southwest shoal. The water depth ranges from 0 to 65 m and rapidly increases to 800–1232 m on the platform slope. The slope reaches 30° at the reef flat front (Figure 2). The lithology and biostratigraphy of the platform have been investigated using two wells (Xiyong-1 and Xichen-1) drilled on Xuande Atoll during the 1980s and well Xike-1 drilled in 2013–2014 (Wang et al., 1979; Xu et al., 2002; Wang et al., 2015).

Four wells have been drilled on Yongxing Island. Wells XY-1, XY-2, XS-1, and XK-1 penetrated up to 1384.68, 600.02, 200.63, and 1268 m, respectively (Figures 1, 2). Based on the wells drilled on Xuande Atoll, the thicknesses of the carbonate platform determined from wells XY-1 and XK-1 are approximately 1275 m and 1251 m, respectively. The Neogene carbonate platform grew on Precambrian or Mesozoic metamorphic and volcanic basement (Zhao et al., 2011), or on Mesozoic metamorphic rocks (152.9 ± 1.7 Ma) and granites (107.8 ± 3.6 Ma) (Zhu et al., 2017). The late Cenozoic platform strata are divided into the Guangle, Xisha, Xuande, Yongle, and Yongxing formations (Figure 3). This stratigraphy was established in the 1990s; however, it has many issues related to the drilling locations and the lack of good chronology data

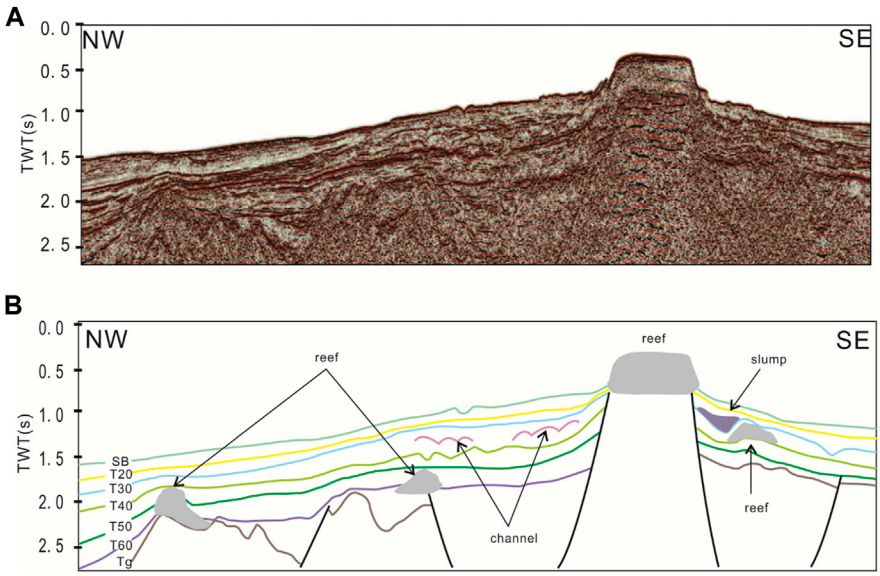

FIGURE 3
Seismic sequence stratigraphy across the Xisha Uplift in the South China Sea. **(A)** Uninterpreted and **(B)** interpreted sections. SB is the seafloor reflector, and T20, T30, T40, T50, and T60 represent the bottom of the Quaternary, Pliocene, Late Miocene, Middle Miocene, and Early Miocene, respectively. Seismic reflector Tg is the acoustic basement reflection.

(Zhao et al., 2011; Zhu et al., 2015). Data from well XK-1 improved the stratigraphy in the region by integrating geochronological information from magnetostratigraphy and astronomical tuning as the age-depth model of well XK-1 has been calibrated (Yi et al., 2018). Based on the model, the bottom ages of the Sanya, Meishan, Huangliu, Yinggehai, and Ledong formations were determined to be 24.3, 16.6, 10.4, 5.7, and 2.2 Ma, respectively.

Data and methods

Seismic surveys were performed onboard the R/V *NH503* from 31 August to 6 September 2017. This was the first seismic experiment across a shallow carbonate platform in the SCS. The acoustic signals were generated by two clustered GI-guns with a maximum of around 210 in^3 and included frequencies of 40–2000 Hz, with the dominant frequencies centred at 150–200 Hz. The seismic signals were received by a GEO-Sense 48 receiver (Netherlands) with an offset of 9.5 m. The sampling interval was 0.25 m, and the vertical resolution reached 2 m. The streamer was 600 m in length, with a 6.25 m channel distance. The source distance was 12.5 m; therefore, the seismic system had a 90 m migration distance and a 24 m overlap. Seismic data processing was performed using the GeoCluster 6100 software package. The key processing steps included: 1) muting using the frequency panel to reduce random noise, Radon transform, and common migration offset distances; 2) suppressing multiple reflections using surface-related multiple elimination (SRME) and prediction deconvolution; 3) velocity analyses, including precision velocity analysis and migration velocity scanning; 4) remaining multiple wave suppression with spectral and static plots; 5) Kirchhoff pre-stack time migration, particularly migration offsets of the aperture and angle; and 6) pre-stack muting to obtain the true amplitude section. Data interpretation was performed using sequence stratigraphic methods. The original seismic data were interpreted using Geoframe 2012. All vertical scales used for the seismic profiles shown herein were two-way travel times. The seismic data were then used to investigate the subsurface structure and sedimentary characteristics of the platform.

Multi-beam bathymetric and single-channel seismic data collected by the Guangzhou Marine Geological Survey (GMGS) were used to image the slopes of the Xisha archipelago. A bathymetric map of the archipelago was constructed from the multi-beam depth soundings combined with satellite data. Multi-beam bathymetry data acquired with a SeaBeam 2112 system (USA) were used to analyse the geomorphology of the archipelago. The multi-beam data were processed using navigation filtering, parameter calibration, transducer draft correction, sound velocity correction, and data filtering (Chen et al., 2015). A 100 m × 100 m cell size was used for the raster grids in this study, with a vertical resolution of 3% of the water depth.

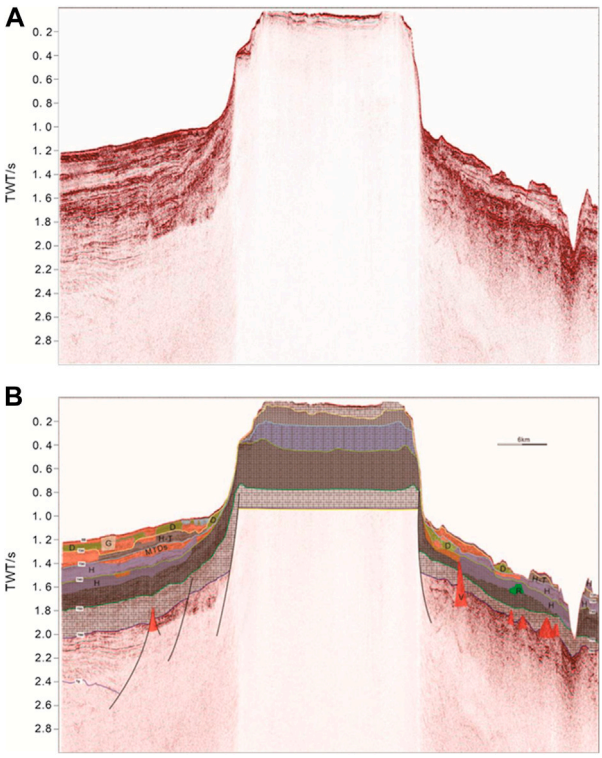

FIGURE 4
(A) Original and **(B)** interpreted sections of the seismic profile XDS05.

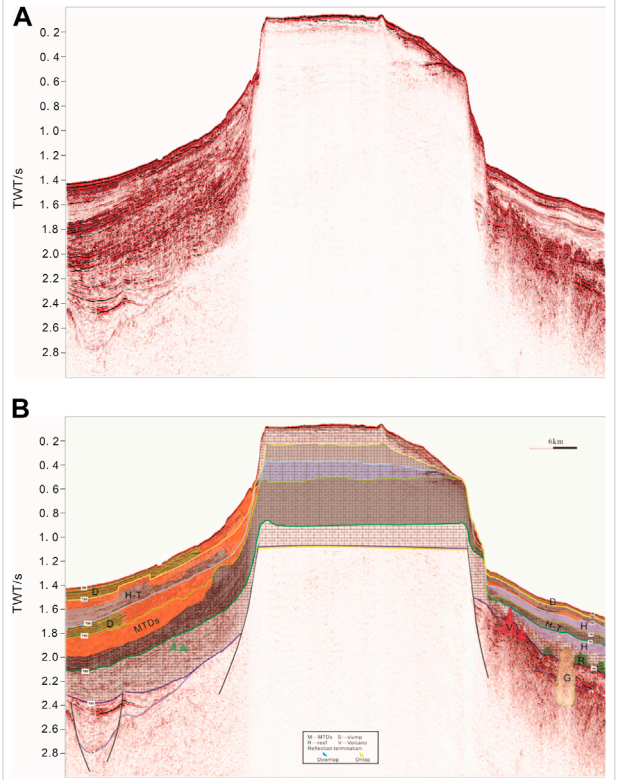

FIGURE 5
(A) Original and **(B)** interpreted sections of the seismic profile XDS01.

Results and interpretation

Modern carbonate platforms exhibit high-amplitude, parallel, and continuous reflections on their tops, and low-amplitude reflections in their internal regions above the basement (Figures 4–7). Six key reflectors were identified in the seismic profile across the platform. Reflector T0 is a seafloor reflector that images the morphology of the platform. T0 shows the flat on the platform and steep slopes on the margins of the platform (Figure 1). Reflector T20 represents the bottom of the Quaternary strata. Reflectors T30 (bottom of the Pliocene), T40 (bottom of the late Miocene), and T50 (bottom of the middle Miocene) represent the bases of different strata, while Tg is a reflector of the acoustic basement that varied in amplitude and frequency, occurring as an undulating interface reflector. According to the reflectors, the reef carbonate strata can be divided into six seismic sequences: SQ1 (early Miocene), SQ2 (middle Miocene), SQ3 (late Miocene), SQ4 (Pliocene), and SQ5 (Quaternary) from the basement to the seafloor (Figures 4–7).

SQ1 is located above the acoustic basement and is characterised by parallel and sub-parallel seismic reflections (Figures 4–6). The reflections onlap the basement high and have complex inner reflections in the eastern part of profile 05 (Figure 4). During the early Miocene, the Xisha uplift was drowned because of marine inundation, and reef carbonates grew on the basement high. During the beginning of the early Miocene, shallow water carbonate deposits formed on the slopes of Xuande Atoll (Figures 6–8). The reef platform was lateral and grew vertically during the early Miocene. Thus, reef carbonates are widely distributed on Xuande Atoll and in adjacent areas (Figures 6–8).

SQ2 represents middle Miocene carbonate strata and is characterised by parallel and sub-parallel seismic reflections in the western part of the profile (Figure 7). However, SQ2 has complex mound-shaped cluttered and wavy divergent reflections in the eastern part of the profile (Figure 8). During the middle Miocene, reef carbonates formed on the leeward slope of the basal uplift and started to grow on the windward slope in the eastern part. These carbonate sequences were deposited on the platform during a stable sea level period. During the late middle Miocene, the sea level increased rapidly, and the carbonate platform migrated accordingly. A pinnacle reef formed on the western slope of the atoll, whereas a wavy drift occurred on the eastern slope. The carbonate platform was only aggraded at Xuande Atoll, whereas deepwater gravity flow deposits, including mass transport deposits (MTDs), formed in the peri-platform area (Figure 8).

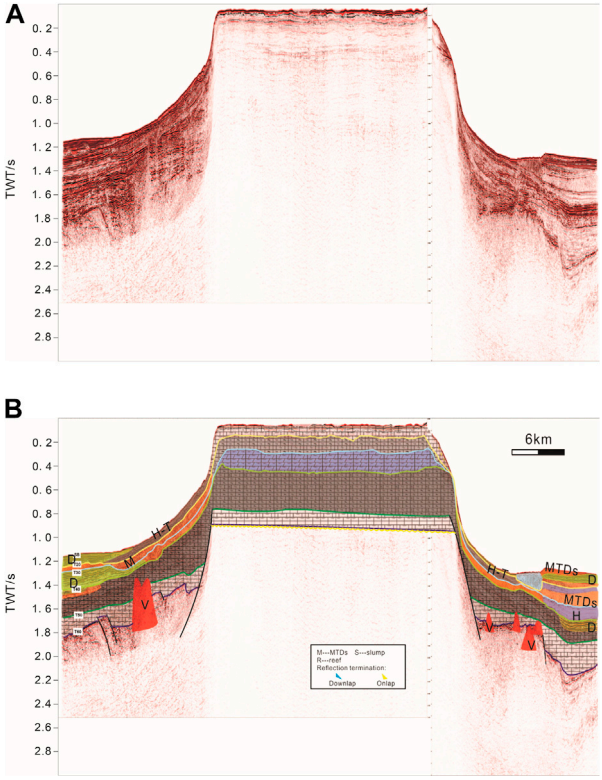

FIGURE 6
(A) Original and **(B)** interpreted sections of the seismic profile XDS10.

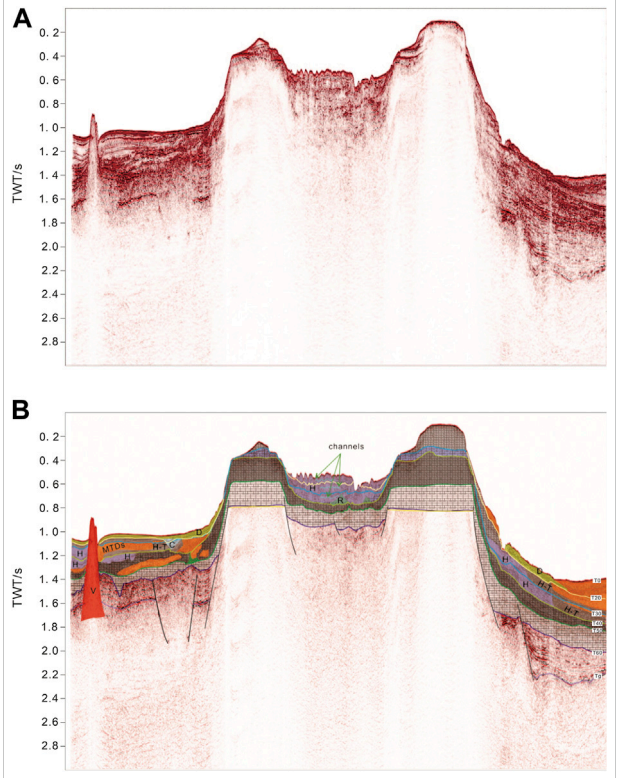

FIGURE 7
(A) Original and **(B)** interpreted sections of the seismic profile XDS11.

SQ3 represents late Miocene carbonate strata and is characterised by parallel and sub-parallel seismic reflections on both sides of the profile (Figure 7). SQ3 also contains S-type reflection structures in the peri-platform area. The reef carbonates grew favourably at Xuande Atoll, owing to rapid subsidence (Figures 5, 6). However, reef growth did not occur in the peri-platform area. The last apparent shrinkage of the platform occurred northward and eastward at the end of the Miocene (Figure 9).

SQ4 represents Pliocene carbonate strata and is characterised by parallel and sub-parallel seismic reflections on both sides of the profile. During the Pliocene, the carbonate platform was limited at the atoll. SQ5 represents Quaternary carbonate strata and is characterised by parallel and sub-parallel seismic reflections on both sides of the profile (Figures 6, 7). High-amplitude chaotic reflections were observed on the slope of the atoll, which could represent bottom current deposits around the atoll (Figure 8). Most of the seafloor around the atoll is covered by hemipelagic sediment, and the slopes contain tidal channels or gullies (Figures 7, 8). The platform margin regressed by 8 km, and the platform decreased from the 300 m to the 60 m isoline, after which the sea level rose and lateral aggradation occurred on the eastern margin of the atoll.

Discussion

Evolution of the Xuande Atoll

The Xisha uplift was undergoing rifting and erosion during the Paleogene. During the early Miocene, coral reef carbonates covered the rapidly subsiding basement in the Xisha region, which covered most of the Xisha uplift located on the continental margin and captured little terrigenous sediment (Wu et al., 2014). Later, the bioherms of the Xisha Islands aggraded and prograded, forming the large shallow carbonate deposits observed in the seismic profiles (Figures 4–7), including the reef flat and interbedded lagoon-beach facies that were also observed in well XK-1 (Shao et al., 2017; Wu et al., 2020).

During the early and late middle Miocene, the rising sea level decelerated and then decreased (Shao et al., 2017). The carbonates in well XK-1 exhibited reef-beach facies, owing to prevailing corrosion and leaching processes in a mixed meteoric water-marine environment (Shao et al., 2017). In the early middle Miocene, shallow carbonate sequences were observed at Xuande Atoll (Figures 6, 7). The shallow carbonate deposits were distributed throughout the Xisha area (Ma et al., 2011). The

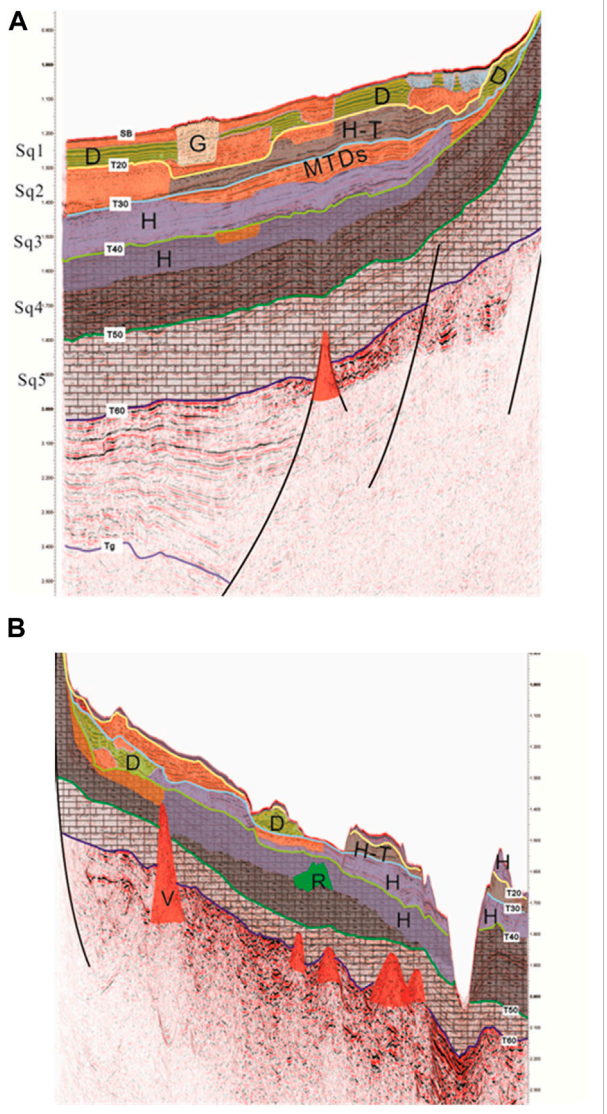

FIGURE 8
(A) Western and **(B)** eastern slopes of the seismic profile XDS05.

peri-platform facies then changed to deepwater facies, indicating that the carbonate platform became isolated during the late middle Miocene (Figure 10).

During the late Miocene, the isolated platform continued to aggrade. Then, when the sea level increased again from the late Miocene to the Pliocene (Shao et al., 2017), the atoll reef terraces extended more broadly and were dominated by lagoon and reef flat facies on their inner sides. However, the platform shrank on the eastern and northern margins (Figure 9). Throughout the Pleistocene, the sea level decreased from its maximum and oscillated with a few deviations. As a result, the carbonate platform on which well XK-1 is located was eroded by freshwater diagenesis. Strata with overbedded reef and beach facies were widely produced, except for patchy carbonates preserved in relatively better conditions (Figure 10). As the upward growth rate of a carbonate platform fails to keep pace with the rates of subsidence or sea level rise, most of the pre-existing reefs and carbonate platforms will become drowned, leaving only the atoll reefs circled topographic highs to continue developing vertically (Hallock and Schlager, 1986; Belopolsky and Droxler, 2003). Such reefs grew rapidly at Xuande Atoll, and some biohermal clasts eroded by ocean waves were deposited around the reefs, partly conveyed downslope by small channels (Figure 4). Atoll reefs developed mainly around the reef islands on the Xisha uplift, represented by the Xuande and Yongle atoll reefs. The Xuande isolated platform underwent slight asymmetric development (Figure 11). The reef flats grew in the north and east, with discontinuity in the south and west (Figures 1, 4, 5, 11). Patch reefs also formed in the lagoon. Apparent platform shrinkage then occurred northward and eastward at the end of the Miocene (Figure 9).

Stratigraphic sequence

The exposed surface of an isolated carbonate platform may represent a seismic boundary at low sea levels. Six exposed surfaces were observed in the carbonate sequences of Xuande Atoll, which formed during gentle decreases in sea level (Figures 4–9). These exposed surfaces usually occurred with dissolution and highly developed porosity and caves, which generally occur in red algal limestones (Zhu et al., 2015). Falling-stage systems tracts (FSTs) could also act as markers of sequence boundaries, which formed highstand tracts (Schlager and Warrlich, 2010). The seismic profiles of Xuande Atoll showed FSTs on the northeastern margin.

The application of the FST model to the margin of the atoll has been discussed in recent years (Schlager and Purkis, 2013). Boundaries in the FST model have been proposed and indicate stratigraphic forward modelling. Comparisons with previous studies have been used to determine the controls and stability domains of two conceptual models concerning relative decreases in sea level in carbonate sequence stratigraphy. In the standard model, deposition occurs during increasing and stable relative sea level stands, whereas a continuous erosional unconformity develops during decreases in sea level. The FST model postulates that significant deposition occurs during decreases in sea level. Sedimentological principles, numerical models, and previous studies of tropical carbonate sequences indicate that the presence or absence of an FST is not simply a function of the rate of the decreasing sea level but rather depends on the balance of the erosion, decreasing sea level, and carbonate production rates. Previous studies plotted in the parameter space support the modelling results. The range of rates required for the FST is common in the geologic records. Consequently, the FST can be expected to be more common around the Xuande Atoll (Figures 7, 8).

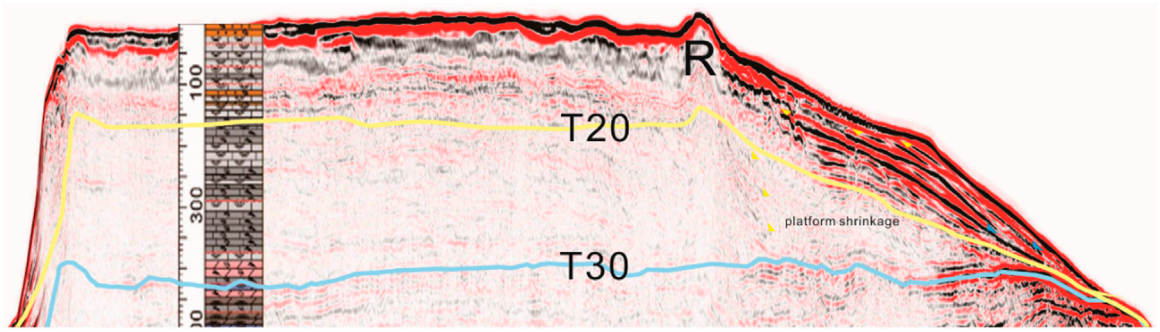

FIGURE 9
Interpreted seismic profile XDS01, showing platform shrinkage at the end of the Miocene.

Mechanisms for platform drowning

The earliest platform drowning event occurred at 15.5 Ma in the latest early Miocene, which included decreased carbonate production and increased water depth (Figure 8). The microfacies of the XY-1 and XK-1 wells at depths of 1000–1100 m included *in situ* corals and coral fragments in the low section, whereas the middle and upper sections were dominated by coralline algae and foraminifera, respectively (Ma et al., 2018). Biological studies have suggested that corals are the most successful benthic carbonate producers in oligotrophic environments but are not competitive in more nutrient-rich water (Hallock and Schlager, 1986; Mutti and Hallock, 2003; Wilson, 2008; Roger et al., 2012). Coral is symbiotic with zooxanthellae (Dubinsky and Falkowski, 2011). Increased nutrient levels stimulate plankton blooms, thereby reducing water transparency and inhibiting the photosynthesis of the zooxanthellae, which limits coral growth (Hallock and Schlager, 1986; Mutti and Hallock, 2003). Subsequently, coralline algae likely occurred in the middle section in response to variations in nutrient levels (i.e., from oligotrophic to mesotrophic conditions) (Hallock et al., 1991; Esteban, 1996; Fournier et al., 2005; Sattler et al., 2009; Lüdmann et al., 2018). In the upper section, coralline algae were gradually replaced by large benthic foraminifera (Ma et al., 2018), including Lepidocyclina and Miogypsina, which represents a eutrophic environment (Hallock et al., 1991; Sattler et al., 2009). Synchronous similar sedimentary microfacies during the drowning of carbonate platforms have been observed on the Liuhua and Malampaya carbonate platforms in the SCS (Fournier et al., 2005; Sattler et al., 2009). The vertical succession of sedimentary microfacies from *in situ* corals to coralline algae and foraminifera was not only a response to continuous increases in nutrient levels but also reflects the deepening of the depositional environment as the Lepidocyclina–Miogypsina requires a deep and low energy environment (Hallock and Schlager, 1986; Geel, 2000; Halfar and Mutti, 2005). As the water depth increased, the high electrical resistance in this section reflected an increasingly muddy component. Carbonate platform drowning is defined by accumulation rates that fail to keep pace with long-term subsidence and sea level changes. The high production of a coral reef can easily keep up with sea level fluctuations, whereas coralline algal growth is much slower. Consequently, we concluded that increased nutrient levels caused production on the Xisha platform to fail to keep pace with subsidence (Wu et al., 2014), resulting in the drowning of the platform in the late early Miocene. While temperature changes may have also affected reef growth, temperature alone cannot change the style of reef builders (Hallock and Schlager, 1986; Sattler et al., 2009). Furthermore, the temperatures during the late early Miocene were relatively stable; thus, temperature was not likely a decisive factor. This temperature analysis was similar to that of the adjacent coeval platform demise in the Dongsha Sea region.

The most important platform drowning event occurred in the late Miocene (10.5–8.2 Ma), which corresponded to the formation of a semi-marginal sea (Li et al., 2014). The sedimentary microfacies in the two wells contained *in situ* corals in the lower section, an algally (Halimeda) dominant middle section, and a foraminiferally dominant upper section (Figure 2). Based on analyses of these sedimentary microfacies associated with slow subsidence, weak eustatic fluctuations, and slightly decreasing temperatures (Wu et al., 2014), we inferred that increased nutrient levels caused the Xisha platform to drown again in the early late Miocene.

Tectonic subsidence

The global sea level fluctuation was around 40 m in the Miocene; however, the thickness of the Miocene carbonate succession in XK-1 is nearly 1 km (Yi et al., 2018), suggesting that an accommodation space created by tectonic subsidence was the main reason for platform growth. The relative sea level is directly linked to carbonate production in carbonate depositional

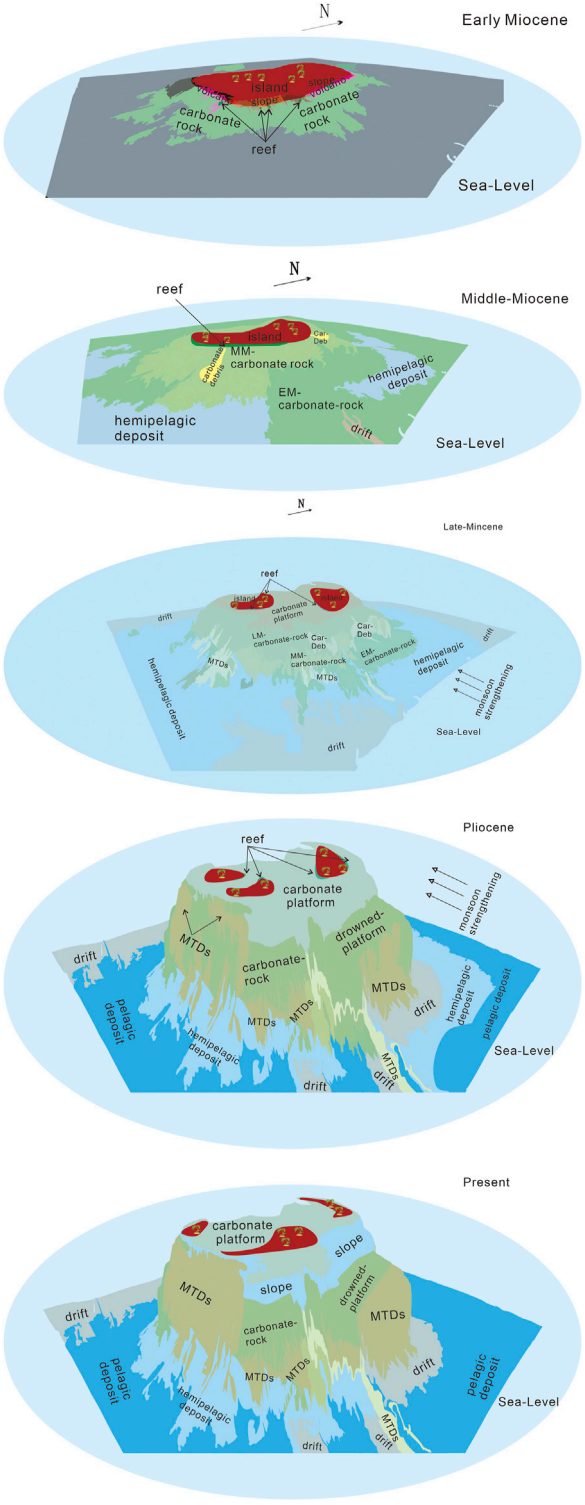

FIGURE 10
Model of the development of Xuande Atoll in the Xisha archipelago.

systems (Tucker and Wright, 2009). Carbonate production is high when a large area of shallow water is available; however, if this area is reduced, the production decreases (Tucker and Wright, 2009). More than 1 km-thick carbonate succession since the Early Miocene indicates the higher accommodation space related to relative sea-level change caused by tectonic subsidence. The subsidence during the early Miocene was 1.0–1.5 km in the deep-water area. The total subsidence was <2 km in the northern Qiongdongnan Basin, which is similar to the results obtained from the wells in this area (Xie et al., 2008; Wu et al., 2014; Shi et al., 2017). Owing to low sediment inputs and the palaeo-water depth, the tectonic subsidence of the Xisha and Guangle uplifts cannot be accurately restored.

Stretching and thinning of lithospheric mantle and crust are commonly considered the primary reason for the subsidence of passive continental margin rift basins, as confirmed by the imitation of crust stretching in the north margin of the South China Sea (Cui et al., 2008; Tong et al., 2009). The mechanism driving crustal extension remains controversial between two factors: dominant extrusion of the Indochina Block and sinistral motion on the Red River Fault Zone (Tapponnier et al., 1982a; Tapponnier et al., 1982a; Briais et al., 1993a; Briais et al., 1993b; Leloup et al., 2001) or the subduction of a proto-SCS in the North Borneo Trench (Taylor and Hayes, 1980; Hall, 2002).

Platform development associated with East Asian monsoons

The reef builders of the Xuande platform were dominantly corals, algae, and other benthic organisms (Wu et al., 2019), which were limited by the maximum depth at which photosynthesis can occur (~100 m) (Riding, 2000a; Woodroffe and Webster, 2014).

During the Miocene, the prevailing summer wind is the East Asian summer monsoon (Clift et al., 2014). Therefore, the wind-driven surface currents and upwelling created a favourable environment for reef growth in the Xisha region. The warm summer wind satisfied the temperature requirement for the reefs. With wind-driven southwest to northeast surface currents, the intense wave action was concentrated on the windward side of the Xisha platform, which is where the reefs were centralised. As the reefs grew, reef detritus accumulated on the foreslope and formed biohermal clasts, some of which were transported by the surface currents to the leeward side of the platform and formed shoal deposits.

In addition, nutrient levels trigged by upwelling would have diffused throughout the platform by the southwestern surface current, which may have induced further reef development on

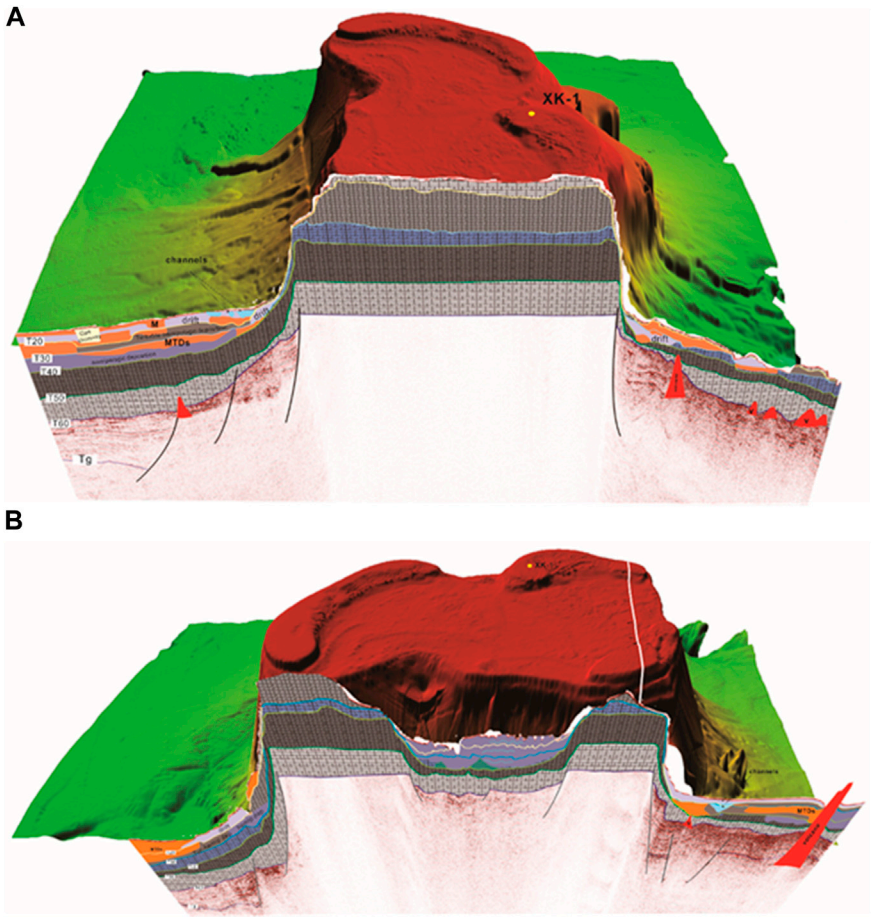

FIGURE 11
Asymmetric development of the Xuande isolated carbonate platform determined from seismic imaging. **(A)** E–W sedimentary model across the entire atoll. **(B)** N–S sedimentary model across the western margin of the atoll.

the southwestern part of the platform. The scale and growth rate of reefs in moderate nutrient content regions are greater than in other parts of the SCS (Su et al., 2006); however, high nutrient contents can lead to reef demise (Hallock and Schlager, 1986; Fournier et al., 2005; Sattler et al., 2009). Wu et al. (2019) reported a change in carbonate factory during the Miocene, which was related to the intensification of summer monsoons. A relationship between nutrient-level-related monsoons and platform partial drowning was reported in the Maldives (Betzler et al., 2018). This relationship requires confirmation on the Xuande platform (Qin et al., 2022).

Conclusion

This study conducted high-resolution seismic surveys of Xuande Atoll in the Xisha archipelago, which identified six seismic reflectors. The results showed that the late Cenozoic carbonate strata on the isolated platform can be divided into five sequences (SQ1, SQ2, SQ3, SQ4, and SQ5). The platform isolation started in the early Miocene, and the platform flourished in the middle Miocene. However, the platform decreased since the late Miocene. During the earliest Quaternary, the platform regressed by 8 km. Late aggradation and lateral regression occurred in the latest Pliocene, which may have been related to the strength of the East Asian monsoon, rapid subsidence, and increased nutrient levels in the northern SCS. The platform slopes were characterised by gravity flows and bottom current deposits. Tectonic events were likely the most important factors in the evolution of the platform, along with terrigenous sediment inputs. The uplift of the Indo-China Peninsula and the formation of the semi-closed SCS increased terrigenous sediment inputs and were unfavourable to reef growth.

Author contributions

YL drafted the manuscript; SW and CY conceived the study; XHu, XL, XHa, and YQ contributed significantly to data analysis and manuscript preparation; WC, JS, LZ, and ZY helped perform data analysis and provided constructive discussions. All authors read and approved the final manuscript.

Funding

Financial support was received from the specific research fund of the Innovation Platform for Academicians of Hainan Province, the National Science Foundation of China (No. 91228208), the International Cooperation Project of Hainan Science and Technology Bureau (No. SQ2016KJHZ0027), and the Hainan Provincial Joint Project of Sanya Yazhou Bay Science and Technology City (420LH029).

Acknowledgments

The authors thank the captain and crew of the R/V *NH503* for their assistance with the seismic data acquisition.

Conflict of interest

The authors declare that the research was conducted in the absence of any commercial or financial relationships that could be construed as a potential conflict of interest.

Publisher's note

References

Belopolsky, A., and Droxler, A. (2003). Imaging Tertiary carbonate system-the Maldives, Indian Ocean: Insights into carbonate sequence interpretation. *Lead. Edge* 22, 646–652. doi:10.1190/1.1599690

Betzler, C., Eberli, G. P., Lüdmann, T., Reolid, J., Kroon, D., Reijmer, J. J. G., et al. (2018). Refinement of Miocene sea level and monsoon events from the sedimentary archive of the Maldives (Indian Ocean). *Prog. Earth Planet. Sci.* 5 (1), 5–18. doi:10.1186/s40645-018-0165-x

Betzler, C., Hubscher, C., Lindhorst, S., Reijmer, J. J. G., Romer, M., Droxler, A. W., et al. (2009). Monsoon-induced partial carbonate platform drowning (Maldives, Indian Ocean). *Geology* 37, 867–870. doi:10.1130/g25702a.1

Briais, A., Patriat, P., and Tapponnier, P. (1993b). Updated interpretation of magnetic anomalies and seafloor spreading stages in the South China Sea: Implications for the Tertiary tectonics of Southeast Asia. *J. Geophys. Res.* 98, 6299–6328. doi:10.1029/92jb02280

Briais, A., Patriat, P., and Tapponnier, P. (1993a). Updated interpretation of magnetic-anomalies and sea-floor spreading stages in the South China sea - implications for the tertiary tectonics of southeast-asia. *J. Geophys. Res.* 98, 6299–6328. doi:10.1029/92jb02280

Chen, J., Song, H., Guan, Y., Yang, S., Pinheiro, L. M., Bai, Y., et al. (2015). Morphologies, classification and Genesis of pockmarks, mud volcanoes and associated fluid escape features in the northern Zhongjiannan Basin, South China Sea. *Deep Sea Res. Part II Top. Stud. Oceanogr.* 122, 106–117. doi:10.1016/j.dsr2.2015.11.007

Clift, P. D., Wan, S., and Blusztajn, J. (2014). Reconstructing chemical weathering, physical erosion and monsoon intensity since 25 Ma in the northern South China sea: A review of competing proxies. *Earth. Sci. Rev.* 130, 86–102. doi:10.1016/j.earscirev.2014.01.002

Cui, T., Xie, X., Ren, J., and Zhang, C. (2008). Dynamic mechanism of anomalous post-rift subsidence in the Yinggehai Basin. *Eart. Scie.* 33, 349–356. doi:10.3799/dqkx.2008.046

Cullen, A. B. (2010). Transverse segmentation of the baram-balabac basin, NW Borneo: Refining the model of borneo's tectonic evolution. *Pet. Geosci.* 16, 3–29. doi:10.1144/1354-079309-828

Dubinsky, Z., and Falkowski, P. (2011). "Light as a source of information and energy in zooxanthellate corals," in *Coral reefs : An ecosystem in transition* (Dordrecht Netherlands: Springer), 107–118.

Eberli, G. P., and Ginsburg, R. N. (1987). Segmentation and coalescence of cenozoic carbonate platforms, northwestern Great Bahama Bank. *Geol.* 15, 75–79. doi:10.1130/0091-7613(1987)15<75:sacocc>2.0.co;2

Esteban, M. (1996). *An overview of Miocene reefs from mediterranean areas: General trends and facies models*. Tulsa, Oklahoma: SEPM Society for Sedimentary Geology.

Fournier, F., Borgomano, J., and Montaggioni, L. F. (2005). Development patterns and controlling factors of Tertiary carbonate buildups: Insights from high-resolution 3D seismic and well data in the Malampaya gas field (Offshore Palawan, Philippines). *Sediment. Geol.* 175, 189–215. doi:10.1016/j.sedgeo.2005.01.009

Fournier, F., Montaggioni, L., and Borgomano, J. (2004). Paleoenvironments and high-frequency cyclicity from cenozoic south-east Asian shallow-water carbonates: A case study from the oligo-miocene buildups of Malampaya (offshore palawan, Philippines). *Mar. Petroleum Geol.* 21, 1–21. doi:10.1016/j.marpetgeo.2003.11.012

Geel, T. (2000). Recognition of stratigraphic sequences in carbonate platform and slope deposits: Empirical models based on microfacies analysis of palaeogene deposits in southeastern Spain. *Palaeogeogr. Palaeoclimatol. Palaeoecol.* 155, 211–238. doi:10.1016/s0031-0182(99)00117-0

Halfar, J., and Mutti, M. (2005). Global dominance of coralline red-algal facies: A response to Miocene oceanographic events. *Geol.* 33, 481–484. doi:10.1130/g21462.1

Hall, R. (2002). Cenozoic geological and plate tectonic evolution of SE Asia and the SW pacific: Computer-based reconstructions, model and animations. *J. Asian Earth Sci.* 20, 353–431. doi:10.1016/s1367-9120(01)00069-4

Hallock, P., and Schlager, W. (1986). Nutrient excess and the demise of coral reefs and carbonate platforms. *Palaios* 1, 389–398. doi:10.2307/3514476

Hallock, P., Silva, I. P., and Boersma, A. (1991). Similarities between planktonic and larger foraminiferal evolutionary trends through paleogene paleoceanographic changes. *Palaeogeogr. Palaeoclimatol. Palaeoecol.* 83, 49–64. doi:10.1016/0031-0182(91)90075-3

Jervey, M. (1988). *Quantitative geological modeling of siliciclastic rock sequences and their seismic expression*. Tulsa, Oklahoma: SEPM Society for Sedimentary Geology.

Jovane, L., Figueiredo, J. J. P., Alves, D. P. V., Iacopini, D., Giorgioni, M., Vannucchi, P., et al. (2016). Seismostratigraphy of the ceará plateau: Clues to decipher the cenozoic evolution of Brazilian equatorial margin. *Front. Earth Sci. (Lausanne).* 4, 90. doi:10.3389/feart.2016.00090

Leloup, P. H., Arnaud, N., Lacassin, R., Kienast, J., Harrison, T., Trong, T. P., et al. (2001). New constraints on the structure, thermochronology, and timing of the Ailao Shan-Red River shear zone, SE Asia. *J. Geophys. Res.* 106, 6683–6732. doi:10.1029/2000jb900322

Li, C. F., Li, J. B., Ding, W. W., Franke, D., Yao, Y. J., Shi, H. S., et al. (2015). Seismic stratigraphy of the central South China Sea basin and implications for neotectonics. *J. Geophys. Res. Solid Earth* 120, 1377–1399. doi:10.1002/2014jb011686

Li, J., Fang, X., Song, C., Pan, B., Ma, Y., and Yan, M. (2014). Late Miocene–Quaternary rapid stepwise uplift of the NE Tibetan Plateau and its effects on climatic and environmental changes. *Quat. Res.* 81, 400–423. doi:10.1016/j.yqres.2014.01.002

Lüdmann, T., Betzler, C., Eberli, G. P., Reolid, J., Reijmer, J. J., Sloss, C. R., et al. (2018). Carbonate delta drift: A new sediment drift type. *Mar. Geol.* 401 (98), 98–111. doi:10.1016/j.margeo.2018.04.011

Ludmann, T., Wong, H. K., and Berglar, K. (2005). Upward flow of north pacific deep water in the northern South China sea as deduced from the occurrence of drift sediments. *Geophys. Res. Lett.* 32, L05614. doi:10.1029/2004gl021967

Ma, Y. B., Wu, S. G., Lv, F. L., Dong, D. D., Sun, Q. L., Lu, Y. T., et al. (2011). Seismic characteristics and development of the Xisha carbonate platforms, northern margin of the South China Sea. *J. Asian Earth Sci.* 40, 770–783. doi:10.1016/j.jseaes.2010.11.003

Ma, Z. L., Li, Q. Y., Liu, X. Y., Luo, W., Zhang, D. J., and Zhu, Y. H. (2018). Palaeoenvironmental significance of Miocene larger benthic foraminifera from the xisha islands, south China sea. *Palaeoworld* 27, 145–157. doi:10.1016/j.palwor.2017.05.007

Mitchum, R. M., Jr, Vail, P. R., and Thompson, S., III (1977). Seismic stratigraphy and global changes of sea level, Part 2: The depositional sequence as a basic unit for stratigraphic analysis, Seismic stratigraphy-applications to hydrocarbon exploration. *Mem. Amer. Assoc. Petrol. Geol.* 26, 53–62.

Mutti, M., and Hallock, P. (2003). Carbonate systems along nutrient and temperature gradients: Some sedimentological and geochemical constraints. *Int. J. Earth Sci.* 92, 465–475. doi:10.1007/s00531-003-0350-y

Posamentier, H., and Vail, P. (1988). *Eustatic controls on clastic deposition II—sequence and systems tract models*. Tulsa, Oklahoma: SEPM Society for Sedimentary Geology.

Qin, Y., Wu, S., and Betzler, C. (2022). Backstepping patterns of an isolated carbonate platform in the northern South China Sea and its implication for paleoceanography and paleoclimate. *Mar. Petroleum Geol.* 146, 105927. doi:10.1016/j.marpetgeo.2022.105927

Qiu, X. L., Ye, S. Y., Wu, S. M., Shi, X. B., Zhou, D., Xia, K. Y., et al. (2001). Crustal structure across the xisha trough, northwestern South China Sea. *Tectonophysics* 341, 179–193. doi:10.1016/s0040-1951(01)00222-0

Qiu, X. L., Zeng, G. P., Yi, X. U., Hao, T. Y., Zhi-Xiong, L. I., Priestley, K., et al. (2006). The crustal structure beneath the shidao station on xisha islands of south China sea. *Chin. J. Geophys.* 49, 1565–1575. doi:10.1002/cjg2.984

Riding, R. (2000a). Microbial carbonates: The geological record of calcified bacterial-algal mats and biofilms. *Sedimentology* 47, 179–214. doi:10.1046/j.1365-3091.2000.00003.x

Roger, L. M., Richardson, A. J., McKinnon, A. D., Knott, B., Matear, R., and Scadding, C. (2012). Comparison of the shell structure of two tropical thecosomata (*Creseis acicula* and diacavolinia longirostris) from 1963 to 2009: Potential implications of declining aragonite saturation. *ICES J. Mar. Sci.* 69, 465–474. doi:10.1093/icesjms/fsr171

Sarg, J. (1988). *Carbonate sequence stratigraphy*. Tulsa, Oklahoma: SEPM Society for Sedimentary Geology.

Sattler, U., Immenhauser, A., Schlager, W., and Zampetti, V. (2009). Drowning history of a Miocene carbonate platform (zhujiang formation, south China sea). *Sediment. Geol.* 219, 318–331. doi:10.1016/j.sedgeo.2009.06.001

Schlager, W., and Purkis, S. J. (2013). Bucket structure in carbonate accumulations of the Maldive, Chagos and Laccadive archipelagos. *Int. J. Earth Sci.* 102, 2225–2238. doi:10.1007/s00531-013-0913-5

Schlager, W., and Warrlich, G. (2010). Record of sea-level fall in tropical carbonates. *Basin Res.* 21, 209–224. doi:10.1111/j.1365-2117.2008.00383.x

Shao, L., Cui, Y. C., Qiao, P. J., Zhang, D. J., Liu, X. Y., and Zhang, C. L. (2017). sea-level changes and carbonate platform evolution of the xisha islands (south China sea) since the early Miocene. *Palaeogeogr. Palaeoclimatol. Palaeoecol.* 485, 504–516. doi:10.1016/j.palaeo.2017.07.006

Shi, X., Jiang, H., Yang, J., Yang, X., and Xu, H. (2017). Models of the rapid post-rift subsidence in the eastern Qiongdongnan Basin, South China Sea: Implications for the development of the deep thermal anomaly. *Basin Res.* 29, 340–362. doi:10.1111/bre.12179

Su, R. X., Sun, D. H., Bloemendal, J., and Zhu, Z. Y. (2006). Temporal and spatial variability of the oxygen isotopic composition of massive corals from the South China Sea: Influence of the Asian monsoon. *Palaeogeogr. Palaeoclimatol. Palaeoecol.* 240, 630–648. doi:10.1016/j.palaeo.2006.03.012

Tapponnier, P., Peltzer, G., Dain, A. Y. L., Armijo, R., and Cobbold, P. (1982a). Propagating extrusion tectonics in Asia: New insights from simple experiments with plasticine. *Geol.* 10, 611. doi:10.1130/0091-7613(1982)10<611:petian>2.0.co;2

Taylor, B., and Hayes, D. E. (1980). "Origin and history of the South China sea," in *The Tectonic and geologic evolution of Southeast Asian seas and islands*. Editor D. E. Hayes (Washington, DC, USA: Geophysical monograph series), 27, 23–56.

Tcherepanov, E. N., Droxler, A. W., Lapointe, P., and Mohn, K. (2008). Carbonate seismic stratigraphy of the Gulf of Papua mixed depositional system: Neogene stratigraphic signature and eustatic control. *Basin Res.* 20, 185–209. doi:10.1111/j.1365-2117.2008.00364.x

Tong, D., Ren, J., Lei, C., Yang, H., and Yin, X. (2009). Lithosphere stretching model of deep water in Qiongdongnan basin, northern continental margin of South China Sea, and controlling of the post-rift subsidence. *Acta Geosci. Sin.* 34, 963–974. doi:10.1016/S1003-6326(09)60084-4

Tucker, M. E., and Wright, V. P. (2009). *Carbonate sedimentology*. Hoboken, NJ, USA: John Wiley & Sons.

Vail, P. R., Mitchum, R. M., and Thompson, S. (1977). *Seismic stratigraphy and global changes of sea level, part 3: Relative changes of sea level from coastal onlap*. Tulsa, Oklahoma: American Association of Petroleum Geologists.

Van Wagoner, J., Mitchum, R., Jr, Posamentier, H., and Vail, P. (1987). *Seismic stratigraphy interpretation using sequence stratigraphy: Part 2: Key definitions of sequence stratigraphy*. Tulsa, Oklahoma: American Association of Petroleum Geologists.

Wang, C., He, X., and Qiu, S. (1979). Preliminary study about carbonate strata and micropaleontology of well xiyong-1 in the xisha islands (paracel islands). *Petroleum Geol. Exp.* 1, 23–32.

Wang, Z., Shi, Z., Zhang, D., Huang, K., You, L., Duan, X., et al. (2015). Microscopic features and Genesis for Miocene to Pliocene dolomite in well xike-1, xisha islands. *Earth Sci.* 40, 633–644. doi:10.3799/dqkx.2015.050

Wilson, M. E. J. (2002). Cenozoic carbonates in Southeast Asia: Implications for equatorial carbonate development. *Sediment. Geol.* 147, 295–428. doi:10.1016/s0037-0738(01)00228-7

Wilson, M. E. J. (2008). Global and regional influences on equatorial shallow-marine carbonates during the Cenozoic. *Palaeogeogr. Palaeoclimatol. Palaeoecol.* 265, 262–274. doi:10.1016/j.palaeo.2008.05.012

Woodroffe, C. D., and Webster, J. M. (2014). Coral reefs and sea-level change. *Mar. Geol.* 352, 248–267. doi:10.1016/j.margeo.2013.12.006

Wu, F., Xie, X., Li, X., Betzler, C., Shang, Z., and Cui, Y. (2019). Carbonate factory turnovers influenced by the monsoon (Xisha islands, south China sea). *J. Geol. Soc. Lond.* 176 (5), 885–897. doi:10.1144/jgs2018-086

Wu, S., Chen, W., Huang, X., Liu, G., Li, X., and Betzler, C. (2020). Facies model on the modern isolated carbonate platform in the Xisha Archipelago, South China Sea. *Mar. Geol.* 425, 106203. doi:10.1016/j.margeo.2020.106203

Wu, S. G., Yang, Z., Wang, D. W., Lu, F. L., Ludmann, T., Fulthorpe, C., et al. (2014). Architecture, development and geological control of the Xisha carbonate platforms, northwestern South China Sea. *Mar. Geol.* 350, 71–83. doi:10.1016/j.margeo.2013.12.016

Wu, S., Yuan, S., Zhang, G., Ma, Y., Mi, L., and Ning, X. (2009). Seismic characteristics of a reef carbonate reservoir and implications for hydrocarbon exploration in deepwater of the Qiongdongnan Basin, northern South China Sea. *Mar. Pet. Geol.* 26, 817–823. doi:10.1016/j.marpetgeo.2008.04.008

Xie, X. O., Muller, R. D., Ren, J. Y., Jiang, T., and Zhang, C. (2008). Stratigraphic architecture and evolution of the continental slope system in offshore Hainan, northern South China Sea. *Mar. Geol.* 247, 129–144. doi:10.1016/j.margeo.2007.08.005

Xu, G.-q., Lu, B.-q., and Wang, H.-g. (2002). Drowning event research: Insights from Cenozoic carbonate platforms in northern South China Sea. *JOURNAL-TONGJI Univ.* 30, 35–40. doi:10.1016/j.sedgeo.2009.06.001

Yi, L., Jian, Z., Liu, X., Zhu, Y., Zhang, D., Wang, Z., et al. (2018). Astronomical tuning and magnetostratigraphy of neogene biogenic reefs in xisha islands, south China sea. *Sci. Bull.* 63, 564–573. doi:10.1016/j.scib.2018.04.001

Zhao, Q. A., Wu, S. G., Xu, H., Sun, Q. L., Wang, B., Sun, Y. B., et al. (2011). Sedimentary facies and evolution of aeolianites on shidao island, xisha islands. *Chin. J. Ocean. Limnol.* 29, 398–413. doi:10.1007/s00343-011-0018-6

Zhu, W. L., Xie, X. N., Wang, Z. F., Zhang, D. J., Zhang, C. L., Cao, L. C., et al. (2017). New insights on the origin of the basement of the xisha uplift, south China sea. *Sci. China Earth Sci.* 60, 2214–2222. doi:10.1007/s11430-017-9089-9

Zhu, W., Wang, Z., Mi, L., Du, X., Xie, X., Lu, Y., et al. (2015). Sequence stratigraphic framework and reef growth unit of well Xike-1 from Xisha Islands, South China Sea. *Earth Sci.* 40, 677–687. doi:10.3799/dqkx.2015.055